Progress of Theoretical Physics, Vol. 127, No. 6, June 2012

Symplectic Expression for Chromatic Aberrations

Yuji Seimiya, Kazuhito Ohmi, Demin Zhou,
John W. Flanagan and Yukiyoshi Ohnishi

KEK-Sokendai, Tsukuba 305-0801, Japan

(Received June 27, 2011; Revised April 3, 2012)

Chromatic aberrations characterize how linear optics parameters, including tunes, beta functions, and x-y coupling parameters, depend on momentum deviation. The definition of chromatic aberration is based on static or slowly varying momentum deviations. Linear optics parameters are expanded in terms of momentum deviation; their coefficients are called chromatic aberrations in this paper. The Hamiltonian and a six-dimensional symplectic map, which are taken into account in both betatron and synchrotron motions, are reconstructed using the measured chromatic aberrations. This map can be used to study the effects of chromatic aberrations in beam-beam, space charge, and electron cloud phenomena.

Subject Index: 600, 630

§1. Introduction

In circular particle accelerators, the synchronous and off-momentum particles experience different kick strengths in magnetic elements such as dipoles and quadrupoles. Consequently, the optics parameters such as tune, beta functions, and x-y coupling, need to be extended to address the chromatic effects. In this paper, the amplitudes of chromatic aberrations are regarded as the coefficients of power series of the optics parameters in terms of momentum deviation. In a realistic ring, the optics parameters are measured through beam experiments, in which typically the beam energy is varied by shifting the RF frequency (for example, see Ref. 1)). Indeed, the optics parameters are extracted from the measurement of turn-by-turn positions via monitoring a kicked beam[2),3)] at a certain location, for example, at the interaction point (IP). Further polynomial fitting of the optics parameters in terms of beam energy gives the amplitudes of chromatic aberrations. Finally, modeling of the optics for off-momentum particles is done with a symplectic expression in this paper.

Modern storage rings operate under the presence of disturbances caused by nonlinear collective effects, such as beam-beam, space charge and electron cloud. In order to avoid enhancement of such disturbances and thus achieve high performance, it is essential to control the linear optics parameters. For example, the tuning of linear optics parameters at the IP is absolutely necessary to achieve a high luminosity in e^+e^- colliders, such as KEKB.[4),5)] Moreover, chromatic aberrations induce a spread in the optics parameters and thence increase the widths and strengths of synchro-betatron resonances. It was found that the correction of chromatic aberrations led to a significant increase in the luminosity of KEKB, from 1.7×10^{34} to 2.1×10^{34} $\mathrm{cm}^{-2}\mathrm{s}^{-1}$.[6),7)] Therefore, compressing the chromatic aberrations also proved to be critically important.

Correction of chromatic aberrations, though very important practically, is not a concern of this paper. Indeed, its main purpose is to construct a simple symplectic map for given chromatic aberrations in a storage ring. The map is constructed by making use of a quadratic-form Hamiltonian. As has been demonstrated in Ref. 6), the map is very useful in investigations of the chromatic effects contributing to complex phenomena like beam-beam collisions. Since the chromatic aberrations are measurable parameters, this kind of investigations is valuable in evaluating the degradation of machine performance, such as the loss rate of luminosity of a collider.

The rest of this paper is organized as follows. The fundamental theory and measurement scheme for linear optics in a six-dimensional phase space are firstly reviewed in §2. By extending the conventional linear theory to off-momentum particles, we derive, step by step, the symplectic maps for chromatic aberrations in §3. As an example of applying the symplectic map, the synchro-betatron resonances in the KEKB are simulated using a particle-tracking code. The simulation results as well as comparison with beam experiments are shown in §4. Finally, the whole work is summarized in §5.

§2. Fundamentals of linear optics theory

2.1. *Linear optics parameters*

When observed turn by turn at a certain location s of a ring, the physical coordinates of a particle, $\boldsymbol{x} = (x, p_x, y, p_y, z, \delta)^T$, are transferred by a 6×6 symplectic matrix $M_6(s)$ corresponding to the linear regime. Here the superscript ^{T} denotes the transpose of a matrix or a vector. The periodicity of the system requires that $M_6(s+L) = M_6(s)$, where L is the circumference of the ring. The matrix M_6 operates on $\boldsymbol{x}$ and gives

$$\boldsymbol{x}(s+L) = M_6(s)\boldsymbol{x}(s). \tag{1}$$

The one-turn matrix M_6 contains 21 independent parameters, i.e. 3 tunes ($\mu_{x,y,z} = 2\pi\nu_{x,y,z}$) and 18 linear optics parameters. The subscripts x, y and z respectively denote the horizontal, vertical and longitudinal motion. The tunes are independent of s; however, the other linear optics parameters are functions of s. The matrix M_6 can be written in the general form of

$$M_6 = R_\eta M_{4\times2} R_\eta^{-1}, \tag{2}$$

where R_η is the dispersion matrix defined by

$$R_\eta = \begin{pmatrix} \{1-|R_{\eta,x}|/(1+r_{\eta,0})\}I_2 & R_{\eta,x}S_2R_{\eta,y}^TS_2/(1+r_{\eta,0}) & R_{\eta,x} \\ R_{\eta,y}S_2R_{\eta,x}^TS_2/(1+r_{\eta,0}) & \{1-|R_{\eta,y}|/(1+r_{\eta,0})\}I_2 & R_{\eta,y} \\ S_2R_{\eta,x}^TS_2 & S_2R_{\eta,y}^TS_2 & r_{\eta,0}I_2 \end{pmatrix}, \tag{3}$$

and $M_{4\times2}$ is a matrix parameterized by Twiss and coupling parameters

$$M_{4\times2} = \begin{pmatrix} M_4 & 0_{4\times2} \\ 0_{2\times4} & M_z \end{pmatrix}. \tag{4}$$

In the above matrices, the 4×4 matrix M_4 and 2×2 matrix M_z represent the linear betatron and synchrotron motions, respectively. The quantities $R_{\eta,x}$, $R_{\eta,y}$, S_2, and I_2 are 2×2 matrices defined by

$$R_{\eta,i}=\begin{pmatrix}\zeta_i & \eta_i\\ \zeta_i' & \eta_i'\end{pmatrix},\quad i=x,y, \tag{5}$$

$$S_2=\begin{pmatrix}0 & 1\\ -1 & 0\end{pmatrix},\quad I_2=\begin{pmatrix}1 & 0\\ 0 & 1\end{pmatrix}. \tag{6}$$

The parameter $r_{\eta,0}$ is defined by $r_{\eta,0}=\sqrt{1-|R_{\eta,x}|-|R_{\eta,y}|}$, and $\eta_{x,y},\eta_{x,y}'$ are dispersion functions and their derivatives. The elements of ζ_x, ζ_x', ζ_y and ζ_y' in matrix $R_{\eta,i}$ characterize the tilt of the beam, i.e. $\langle xz\rangle$, $\langle p_xz\rangle$, $\langle yz\rangle$, and $\langle p_yz\rangle$, respectively. In the ring, $\zeta_{x,y}$ and $\zeta_{x,y}'$ are generated in a RF cavity with nonzero dispersion or in a crab cavity, and they vary along s.

The betatron matrix is expressed by[8),9)]

$$M_4=RM_{2\times2}R^{-1}, \tag{7}$$

where the block-diagonal 4×4 matrix $M_{2\times2}$ is the so-called Courant-Snyder matrix expressed by

$$M_{2\times2}=\begin{pmatrix}M_x & 0_2\\ 0_2 & M_y\end{pmatrix} \tag{8}$$

with

$$M_i=\begin{pmatrix}\cos\mu_i+\alpha_i\sin\mu_i & \beta_i\sin\mu_i\\ -\gamma_i\sin\mu_i & \cos\mu_i-\alpha_i\sin\mu_i,\end{pmatrix}, \tag{9}$$

where $i=x,y$. The matrix R characterizes the x-y coupling and is defined by

$$R=\begin{pmatrix}r_0I_2 & -S_2R_2^TS_2\\ -R_2 & r_0I_2\end{pmatrix} \tag{10}$$

with

$$R_2=\begin{pmatrix}r_1 & r_2\\ r_3 & r_4\end{pmatrix}, \tag{11}$$

where $r_0=\sqrt{1-|R_2|}$.[10)] In particular, the matrix $M_{2\times2}$ is parameterized by two betatron tunes (ν_x,ν_y) and 8 linear optics parameters $(\alpha_{x,y},\beta_{x,y},r_i(i=1,...4))$. Similarly, one can show that $\boldsymbol{x}_\beta$ and $\boldsymbol{u}=R^{-1}\boldsymbol{x}_\beta$ are the vectors of the coupled and uncoupled coordinates, respectively.

The synchrotron motion is described by the 2×2 matrix M_z in Eq. (4). M_z has the same form as Eq. (9) with $\beta_z=\alpha_pL/\mu_z$, where α_p is the momentum compaction factor. In this paper, the sign of the synchrotron tune is chosen to be $\mu_z<0$ for $\alpha_p>0$. For storage rings, usually it is true that $\alpha_z\approx0$ with $|\mu_z|\ll1$.

By comparing Eqs. (1) and (2), one can re-express the physical coordinates $\boldsymbol{x}$ as[8)]

$$\boldsymbol{x}=R_\eta\begin{pmatrix}\boldsymbol{x}_\beta\\ \boldsymbol{x}_s\end{pmatrix}, \tag{12}$$

where the coordinates for betatron and synchrotron motions are respectively defined as $\boldsymbol{x}_\beta = (x_\beta, p_{x,\beta}, y_\beta, p_{y,\beta})^T$ and $\boldsymbol{x}_s = (z_s, \delta_s)^T$. It is seen that the matrices $M_{4\times2}$ and M_6 describe the same physical system, except that the coordinates $(\boldsymbol{x}_\beta, \boldsymbol{x}_s)^T$ are transformed into $\boldsymbol{x}$. But the matrix $M_{4\times2}$ has a block-diagonal form resulted from the transformation via R_η. Due to this diagonalization, the motions in the longitudinal and transverse directions are decoupled.

It follows from the above definitions that the synchrotron variables z and δ are expressed by

$$z = \boldsymbol{\eta}^T S_4 \boldsymbol{x}_\beta + r_{\eta,0} z_s, \tag{13}$$

$$\delta = -\boldsymbol{\zeta}^T S_4 \boldsymbol{x}_\beta + r_{\eta,0} \delta_s, \tag{14}$$

where $\boldsymbol{\eta} = (\eta_x, \eta'_x, \eta_y, \eta'_y)^T$ and $\boldsymbol{\zeta} = (\zeta_x, \zeta'_x, \zeta_y, \zeta'_y)^T$. As an example, the relative difference between δ and δ_s is $(\delta - \delta_s)/\delta = 0.15\%$ for the KEKB crab cavity operation with $\zeta_x = 0.011$, horizontal and longitudinal momentum spreads of $\sigma_{p_x} = 10^{-4}$ and $\sigma_\delta = 7 \times 10^{-4}$. The non-zero vector $\boldsymbol{\zeta}$ is also induced by the RF cavity that is located in the dispersive section. But generally $\boldsymbol{\zeta}$ induced by a RF cavity is far smaller than that induced by a crab cavity.

In the literature, the first-order derivative of the tune $\mu(\delta) = 2\pi\nu(\delta)$ over momentum deviation is generally called the chromaticity, i.e.

$$\frac{d\nu(\delta)}{d\delta} = \xi(\delta). \tag{15}$$

In principle, the chromaticity is also function of momentum deviation, and its linear term is $\xi = \xi(0)$. It is natural that other optics parameters related to the betatron motion, i.e. $\beta(\delta)$, $\alpha(\delta)$, and $r_i(\delta)$, also depend on the momentum deviation. These parameters may be expanded in terms of the momentum deviation δ. The coefficients of this expansion are called chromatic aberrations.

In our scheme, betatron-synchrotron variables $(\boldsymbol{x}_\beta, \boldsymbol{x}_s)$ are introduced in Eq. (12). δ_s is more convenient to use than the original momentum deviation δ when discussing symplectic nature. Chromatic aberrations are redefined as the "betatron optics parameters that are functions of δ_s". Note that $\delta = \delta_s$ when $\boldsymbol{\zeta} = 0$, or the difference is small in most of the cases discussed above.

The linear dynamics formalism with 5 variables (x, p_x, y, p_y, δ) is ordinarily used to introduce the betatron variables and the dispersion. In this ordinary formalism, energy is constant; the RF cavity is not taken into account. There are discrepancies between the values obtained by the ordinary formalism and those obtained by our six-dimensional formalism for the Twiss and dispersion parameters when accelerating cavities are present in the dispersive section or the crab cavity. There should be discrepancies between the emittances and chromatic aberrations, which are given by the integrals of the Twiss and dispersion parameters, of the two formalisms. Needless to say, those given by the six-dimensional formalism are correct.

Another type of chromatic aberration can be induced if accelerating cavities are present in the dispersive section or the crab cavity. The physical variables are expressed by the betatron-synchrotron variables, as shown in Eq. (3), as follows:

$$\boldsymbol{x} \approx \boldsymbol{x}_\beta + \boldsymbol{\eta}\delta_s + \boldsymbol{\zeta} z_s. \tag{16}$$

The second and third terms on the RHS contribute to the chromatic aberrations for δ_s and z_s in sextupole magnets. The betatron tune is now expressed by

$$\nu(z_s, \delta_s) = \nu(0,0) + \xi\delta_s + \xi_z z_s + ... \tag{17}$$

The other betatron optics parameters are also expanded by z_s and δ_s. Although the extended chromatic aberrations depending on z_s are not treated in this paper, it is possible to apply our discussion to the chromatic aberrations that depend on both z_s and δ_s.

2.2. *Optics measurement scheme using betatron oscillation*

Before derivations of the symplectic map for chromatic aberrations, it is necessary for us to discuss the optics measurement scheme. As stated previously, one essential advantage of our method is using measurable parameters obtained by beam experiments. If the beam is kicked in a dispersion-free region, it will oscillate in the betatron phase space around the closed orbit.

In the experiments, the beam energy is changed by shifting the frequency of the RF cavity. The closed orbit for the frequency shift Δf is given by

$$M_6\boldsymbol{x} + \boldsymbol{f} = \boldsymbol{x}, \qquad \boldsymbol{f} = (0,0,0,0,\Delta z, 0)^T, \tag{18}$$

where $\Delta z = -L\Delta f/(hf_0)$. The quantities f_0 and h are the RF frequency and harmonic number, respectively. The shifts of δ and δ_s are given by

$$\begin{aligned}\delta = r_{\eta,0}^2\Delta z/(\alpha_p L) - \frac{\Delta z}{2}\Big[&\cot\frac{\mu_x}{2}(\gamma_x\zeta_x^2 + 2\alpha_x\zeta_x\zeta_x' + \beta_x\zeta_x'^2) \\ &+ \cot\frac{\mu_y}{2}(\gamma_y\zeta_y^2 + 2\alpha_y\zeta_y\zeta_y' + \beta_y\zeta_y'^2)\Big],\end{aligned} \tag{19}$$

$$\delta_s = r_{\eta,0}\Delta z/(\alpha_p L), \tag{20}$$

where $(\zeta_x, \zeta_x', \zeta_y, \zeta_y')^T = R^{-1}\boldsymbol{\zeta}$ and $r_{\eta,0}$ are the values at the RF cavity. In most cases, $r_{\eta,0} \approx 1$ and the second term in Eq. (19) is small, and then the difference between δ and δ_s induced by the frequency shift is also small. For example of KEKB ($\zeta_x = 0.011, \beta_x \approx 1$ m), suppose that $r_{\eta,0} = 1$, the second term in Eq. (19) is about 10^{-5} times smaller than the first term. Thus, it is fair to assume that $\delta = \delta_s$, and then the tunes and transverse optics parameters, which are measured as functions of $\Delta z/(\alpha_p L)$, can be regarded as functions of δ_s.

With this simplification, the transfer matrix for the betatron motion is expressed by

$$\begin{aligned}M_4(\delta_s) &= R(\delta_s)\exp\left[\mu_x(\delta_s)S_4A_x(\delta_s) + \mu_y(\delta_s)S_4A_y(\delta_s)\right]R^{-1}(\delta_s) \\ &= \exp\left[\mu_x(\delta_s)S_4R^{-1T}(\delta_s)A_x(\delta_s)R^{-1}(\delta_s) + \mu_y(\delta_s)S_4R^{-1T}(\delta_s)A_y(\delta_s)R^{-1}(\delta_s)\right],\end{aligned} \tag{21}$$

where A_x and A_y are symmetric matrices represented by Twiss parameters, i.e.

$$A_x = \left(\begin{array}{cc|c} \gamma_x & \alpha_x & \\ \alpha_x & \beta_x & 0_2 \\ \hline & 0_2 & 0_2 \end{array}\right), \tag{22}$$

$$A_y = \left(\begin{array}{c|cc} 0_2 & \multicolumn{2}{c}{0_2} \\ \hline 0_2 & \gamma_y & \alpha_y \\ & \alpha_y & \beta_y \end{array}\right). \tag{23}$$

Suppose that $A_i^R = R^{-1T} A_i R^{-1}$ with $i = x, y$, it can be verified that the Courant-Snyder invariants are $2J_i = \boldsymbol{x}_\beta^T A_i^R \boldsymbol{x}_\beta$, since there is

$$\exp\left(-\mu_x A_x^R S_4 - \mu_y A_y^R S_4\right) A_i^R \exp\left(\mu_x S_4 A_x^R + \mu_y S_4 A_y^R\right) = A_i^R, \tag{24}$$

where the relations $\exp(-\mu_{x,y} A_{x,y} S_4) A_{x,y} = A_{x,y} \exp(-\mu_{x,y} S_4 A_{x,y})$ and $A_{x,y} S_4 A_{x,y} = A_{x,y}^R S_4 A_{x,y}^R = 0$ are used. For the given Courant-Snyder invariants $(2J_{x,y})$, the phase space trajectory is expressed by Dirac delta functions, i.e.

$$\delta(\boldsymbol{x}_\beta^T A_x^R \boldsymbol{x}_\beta - 2J_x)\delta(\boldsymbol{x}_\beta^T A_y^R \boldsymbol{x}_\beta - 2J_y). \tag{25}$$

It is obvious that the above function describes a combination of two ellipses (elliptic torus) in a four-dimensional phase space.

The easiest way to determine A_x^R or A_y^R is to measure the second-order moment of the phase space variables. Suppose that a kicker excites the x mode with an amplitude J_x. The second-order moment of the elliptic trajectory is expressed by

$$\langle \boldsymbol{x}_\beta \boldsymbol{x}_\beta^T \rangle = \frac{1}{2\pi} \oint \boldsymbol{x}_\beta \boldsymbol{x}_\beta^T \delta(\boldsymbol{x}_\beta^T A_x^R \boldsymbol{x}_\beta - 2J_x) d\boldsymbol{x}_\beta \tag{26}$$

$$= \frac{1}{2\pi} \oint R\boldsymbol{u}\boldsymbol{u}^T R^T \delta(\gamma_x x^2 + 2\alpha_x x p_x + \beta_x p_x^2 - 2J_x) d\boldsymbol{u} \tag{27}$$

$$= J_x R \left(\begin{array}{cc|c} \beta_x & -\alpha_x & \\ -\alpha_x & \gamma_x & 0_{2\times 2} \\ \hline \multicolumn{2}{c|}{0_{2\times 2}} & 0_{2\times 2} \end{array}\right) R^T. \tag{28}$$

The complete form of $\langle \boldsymbol{x}_\beta \boldsymbol{x}_\beta^T \rangle$ for x and y modes is given in Ref. 3). In beam experiments, the second-order moments $\langle \boldsymbol{x}_\beta \boldsymbol{x}_\beta^T \rangle$ are extracted from data of beam position monitors, and thus Twiss parameters contained in A_x and R are determined.

§3. Symplectic maps for chromatic aberrations

In most of the following we neglect the chromatic aberrations in the dispersion matrix and treat the symplectic maps operating on the dynamic variables $(\boldsymbol{x}_\beta, \boldsymbol{x}_s)^T$ instead of $\boldsymbol{x}$. To demonstrate our method, we start from discussing a simple case of first-order chromatic aberrations for the betatron motion in the horizontal plane in §3.1. Then, in §§3.2 and 3.3, the method is extended to arbitrary chromatic aberrations for Twiss parameters and for x-y coupling, respectively. An alternative approach to constructing a symplectic map for chromatic aberrations is discussed in §3.4. The general expression for the nonlinear dispersion function is addressed in §3.5.

3.1. *Linear chromatic aberrations*

The fundamental concept of our method can be elucidated with the simplest case of linear chromatic aberrations without considering x-y coupling. Suppose that three

Twiss parameters for the horizontal motion are defined by a first-order expansion in terms of δ_s as follows:

$$\begin{aligned}\mu_x &= \mu_{x,0} + \mu_{x,1}\delta_s,\\ \beta_x &= \beta_{x,0} + \beta_{x,1}\delta_s,\\ \alpha_x &= \alpha_{x,0} + \alpha_{x,1}\delta_s,\end{aligned} \tag{29}$$

where the quantities $\mu_{x,1}, \alpha_{x,1}$ and $\beta_{x,1}$ are the first-order chromatic aberrations. The extension to the vertical motion can be obtained easily by replacing x by y in the above equations. For the sake of convenience, however, the subscript x will be dropped in this subsection and §3.2. Furthermore, the subscripts β and s are also left out of both the betatron variables $\boldsymbol{x}_\beta$ and the synchrotron variables $\boldsymbol{x}_s$ in §§3.1−3.4.

The one-turn transfer matrix for betatron motion has the same form as shown in Eq. (9), with μ, α, and β now depending on δ. This expression is symplectic for the x or y motion in its two dimensional phase space, but it is not symplectic in the six dimensional phase space when synchrotron motion is included. Ideally, the map for betatron motion can be written as follows:[11),12)]

$$M(\delta) \equiv \exp\left[(\mu_0 + \mu_1\delta)S_2 \begin{pmatrix} \gamma(\delta) & \alpha_0 + \alpha_1\delta \\ \alpha_0 + \alpha_1\delta & \beta_0 + \beta_1\delta \end{pmatrix}\right], \tag{30}$$

where $\gamma(\delta) = [1+(\alpha_0+\alpha_1\delta)^2]/(\beta_0+\beta_1\delta)$. However, this form is difficult to evaluate in a symplectic manner. Instead, the δ-dependent matrix can be split into the product of two matrices as follows:

$$M(\delta) = M(0)M_H(\delta). \tag{31}$$

The above expression implies that all the chromatic dependences are lumped into $M_H(\delta)$. To find the explicit form of $M_H(\delta)$, it is convenient to use a mixed variable generating function F_2[13)] defined as power series of momentum deviation.

Truncated to the first order terms of momentum deviation, F_2 can be written in the form of

$$F_2(x, \bar{p}, \bar{\delta}) = x\bar{p} + z\bar{\delta} + H_I(x, \bar{p}, \bar{\delta}), \tag{32}$$

where the quadratic Hamiltonian H_I is defined by

$$H_I(x, p, \delta) = \frac{ax^2 + 2bxp + cp^2}{2}\delta, \tag{33}$$

and the quantities $\bar{x}$, $\bar{p}$, $\bar{z}$, and $\bar{\delta}$ are the new coordinates after transformation. Since the generating function should give linear transformation for the betatron motion, F_2 only contains terms of x and p up to the second-order, and the parameters a, b and c are to be determined later.

Using the generation function F_2, the coordinate transformation can be derived by

$$\bar{x} = \frac{\partial F_2}{\partial \bar{p}} = x + \frac{\partial H_I}{\partial \bar{p}} = x + bx\bar{\delta} + c\bar{p}\bar{\delta}, \tag{34}$$

$$p = \frac{\partial F_2}{\partial x} = \bar{p} + \frac{\partial H_I}{\partial x} = \bar{p} + ax\bar{\delta} + b\bar{p}\bar{\delta}, \tag{35}$$

$$\bar{z} = \frac{\partial F_2}{\partial \bar{\delta}} = z + \frac{\partial H_I}{\partial \bar{\delta}} = z + (ax^2 + 2bx\bar{p} + c\bar{p}^2)/2, \tag{36}$$

$$\delta = \bar{\delta}. \tag{37}$$

From the above equations, the new coordinates are transferred by

$$\begin{pmatrix} \bar{x} \\ \bar{p} \end{pmatrix} = M_H(\delta) \begin{pmatrix} x \\ p \end{pmatrix}, \tag{38}$$

with the transfer matrix of

$$M_H(\delta) = \begin{pmatrix} 1 + b\delta - \frac{ac\delta^2}{1+b\delta} & \frac{c\delta}{1+b\delta} \\ -\frac{a\delta}{1+b\delta} & \frac{1}{1+b\delta}. \end{pmatrix}. \tag{39}$$

Equations (36) and (37) show how the symplecticity condition leads to coupling of transverse and longitudinal motions.

The next step is to derive the relations between (a, b, c) and $(\alpha_1, \beta_1, \mu_1)$ defined in Eq. (30). Firstly, $M_H(\delta)$ is solved using Eq. (31)

$$M_H(\delta) = M^{-1}(0)M(\delta). \tag{40}$$

By expanding the right hand side (RHS) of the above equation in terms of δ and comparing its elements with Eq. (39), the coefficients a, b and c can be explicitly determined as follows:

$$\begin{aligned} a = \frac{\sin^2\mu_0}{\beta_0^2} \big[& -\beta_1(\cot\mu_0 + \alpha_0)(1+\alpha_0^2) \\ & + \big\{ -\alpha_1 + \mu_1 \csc^2\mu_0 + 2\alpha_1\alpha_0 \cot\mu_0 \\ & + (\alpha_1 + \mu_1 \csc^2\mu_0)\alpha_0^2 \big\} \beta_0 \big], \end{aligned} \tag{41}$$

$$\begin{aligned} b = \frac{\sin^2\mu_0}{\beta_0} \big[& -\beta_1(1+\alpha_0^2) + \{\alpha_1 \cot\mu_0 \\ & + (\alpha_1 + \mu_1 \csc^2\mu_0)\alpha_0 \big\} \beta_0 \big], \end{aligned} \tag{42}$$

$$c = \big[\beta_1 \cot\mu_0 - \beta_1\alpha_0 + (\alpha_1 + \mu_1 \csc^2\mu_0)\beta_0\big] \sin^2\mu_0. \tag{43}$$

Immediately it is seen that a, b and c are expressed in terms of $(\mu_0, \alpha_0, \beta_0, \mu_1, \alpha_1, \beta_1)$, which are measurable parameters as has been discussed in the previous section.

Once the map given by Eqs. (34)−(37) ($\mathcal{M}_{H_I}$) is achieved, one can construct a one-turn map as follows:

$$R_\eta \circ M_{4\times2}(0) \circ \mathcal{M}_{H_I} \circ R_\eta^{-1}, \tag{44}$$

where R_η is given by Eq. (3). The above map operates on the dynamic variables of $\boldsymbol{x}$. The symbol "$\circ$" in the above equation indicates an operation of product between two maps. At this point, the map is not matrix due to Eq. (36). The operation is

performed from the right to the left. Since the x-y coupling is not taken into account, the coupling matrix R in M_4 (Eq. (7)) is simply a 4×4 unit matrix.

Transformation $\mathcal{M}_{H_I}$ is performed using the energy before RF acceleration in each revolution. The approximation is feasible for a small synchrotron tune; that is, the energy change in one revolution is small.

The transformation given by Eq. (39) contains higher-order terms in δ, this is necessary to maintain the symplectic condition in x motion and y motion. It is noted that if the matrix $M(0)M_H(\delta)$ is used to calculate the Twiss parameters, it does not reproduce the definitions of Eq. (29), but contains leakage to higher-order terms in δ. Figure 1 shows the tune and beta functions as functions of δ given in Eq. (39) at the collision point in the high energy ring (HER) of KEKB, where the Twiss parameters and their linear chromatic aberrations are $\alpha_0 = 0$, $\beta_0 = 1.45$ m, $d\nu/d\delta = 1.3$, $d\beta/d\delta = 45$ m and $d\alpha/d\delta = -18$. The coefficients are $(a, b, c) = (5.0, -0.60, 13.0)$, $(4.3, -1.3, 15.0)$ and $(3.6, -2.1, 16.0)$ for $\nu_0 = 0.505, 0.510$ and 0.516, respectively. It is seen that the leakage to nonlinear terms in δ that appear in Eq. (39) is negligible, but the beta function exhibits significant leakage when the tune approaches the half integer (or an integer). This leakage can be improved by taking into account higher-order terms of δ in the generating function or the Hamiltonian, as to be discussed in the next section.

3.2. *Higher-order chromatic aberrations*

It is straightforward to extend the method demonstrated in the previous section to treat higher-order chromatic aberrations. In a general form, the tune and Twiss parameters are expanded in terms of δ as follows:

$$\begin{aligned}
\mu &= \mu_0 + \sum_{n=1}^{N} \mu_n \delta^n, \\
\beta &= \beta_0 + \sum_{n=1}^{N} \beta_n \delta^n, \\
\alpha &= \alpha_0 + \sum_{n=1}^{N} \alpha_n \delta^n.
\end{aligned} \tag{45}$$

Mathematically the upper band of summations N can be taken to infinity in the above equations, however, high-order chromatic aberrations are hard to be measured accurately. Practically, $N = 2$ or 3 is the reasonable order to be considered.[6)]

Following the treatment in the previous section, the chromatic aberrations are related to the Hamiltonian defined by

$$H_I(x, \bar{p}, \bar{\delta}) = \sum_{n=1} \frac{a_n x^2 + 2b_n x\bar{p} + c_n \bar{p}^2}{2} \bar{\delta}^n. \tag{46}$$

The transformation for the Hamiltonian $M_H(\delta)$ is expressed in the same form as Eq. (39) by replacing $a\delta$, $b\delta$ and $c\delta$ with

$$a\delta \to \sum a_n \delta^n \equiv A,$$

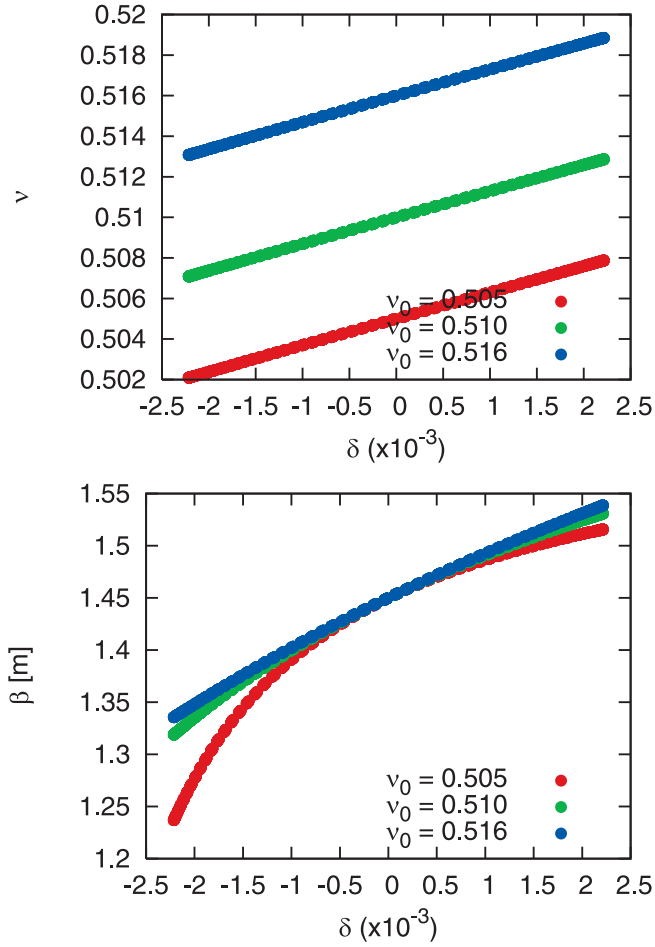

Fig. 1. Tune and beta function as functions of δ given by Eq. (39) at the collision point in KEK-HER, where the linear chromatic aberrations are $d\nu/d\delta = 1.3$, $d\beta/d\delta = 45$ m, and $d\alpha/d\delta = -18$.

$$b\delta \to \sum b_n \delta^n \equiv B,$$
$$c\delta \to \sum c_n \delta^n \equiv C. \tag{47}$$

Consequently, the transfer matrix for chromatic aberrations $M_H(\delta)$ is expressed as

$$M_H(\delta) = \begin{pmatrix} 1 + B - \frac{AC}{1+B} & \frac{C}{1+B} \\ \frac{-A}{1+B} & \frac{1}{1+B} \end{pmatrix}. \tag{48}$$

The transformation for z is

$$\bar{z} = z + \sum_{n=1} (ax^2 + 2bx\bar{p} + c\bar{p}^2) n\delta^{n-1}/2. \tag{49}$$

The relations between $(\mu_n, \beta_n, \alpha_n)$ and (a_n, b_n, c_n) can be obtained by equalizing the matrices defined by Eqs. (40) and (48).

For example, the second-order relations are given as follows:

$$\begin{aligned} a_2 = \frac{1}{2\beta_0^2}\big[&2a_1b_1\beta_0^2 + \{(-\alpha_2\cos 2\mu_0 + \alpha_2 + 2\mu_2 \\ &+ \alpha_1\mu_1\sin 2\mu_0)\alpha_0^2 + 2(b_1^2 - a_1c_1 + \mu_1(\alpha_1 + \mu_1) \\ &+ \alpha_1\mu_1\cos 2\mu_0 + \alpha_2\sin 2\mu_0)\alpha_0 - \alpha_2 + 2\mu_2 \\ &+ \alpha_2\cos 2\mu_0 + 2(b_1^2 + \mu_1^2 - a_1c_1)\cot\mu_0 \\ &- \alpha_1\mu_1\sin 2\mu_0\}\beta_0 - 2(\beta_1\mu_1\cos\mu_0 \\ &+ \beta_2\sin\mu_0)(\cos\mu_0 + \alpha_0\sin\mu_0)(\alpha_0^2 + 1)\big], \end{aligned} \tag{50}$$

$$\begin{aligned} b_2 = \frac{1}{2\beta_0}\big[&\{2b_1^2 + \mu_1(\alpha_1 + \mu_1) + \alpha_1\mu_1\cos 2\mu_0 \\ &+ \alpha_2\sin 2\mu_0 + (-\alpha_2\cos 2\mu_0 + \alpha_2 + 2\mu_2 \\ &+ \alpha_1\mu_1\sin 2\mu_0)\alpha_0\}\beta_0 - 2(\beta_1\mu_1\cos\mu_0 \\ &+ \beta_2\sin\mu_0)(\alpha_0^2 + 1)\sin\mu_0\big], \end{aligned} \tag{51}$$

$$\begin{aligned} c_2 = \frac{1}{2}\big[&2b_1c_1 + \beta_1\mu_1 - \beta_2\alpha_0 + \alpha_2\beta_0 \\ &+ 2\mu_2\beta_0 + (\beta_1\mu_1 + \beta_2\alpha_0 - \alpha_2\beta_0)\cos 2\mu_0 \\ &+ (\beta_2 - \beta_1\mu_1\alpha_0 + \alpha_1\mu_1\beta_0)\sin 2\mu_0\big]. \end{aligned} \tag{52}$$

It is seen that the the above formula contain chromatic aberrations up to the second-order, although they contain terms of third (and higher) order for δ. Higher-order parameters of (a_n, b_n, c_n) can be obtained in a similar way, however, they are not provided here because the expressions are very lengthy.

3.3. *Chromatic aberrations related to X-Y coupling*

In this section, we take into account the x-y coupling in the betatron motion represented by the 4×4 matrix M_4. The parameterization of the x-y coupling is given in Eqs. (7)–(11). The matrix M_4 defined in Eq. (7) should now be regarded as a function of δ such that

$$M_4(\delta) = R(\delta)M_{2\times 2}(\delta)R^{-1}(\delta). \tag{53}$$

The momentum-dependent coupling parameters can be expanded as

$$r_i(\delta) = r_{i,0} + \sum_{n=1} r_{i,n}\delta^n, \tag{54}$$

where the coefficients $r_{i,n}$ are regarded as the chromatic aberrations for x-y coupling.

With x-y coupling included, the Hamiltonian resulted from the chromatic aberrations is expressed as

$$H_I(x, \bar{p}_x, y, \bar{p}_y, \bar{\delta})$$

$$
\begin{aligned}
&= \sum_{n=1} (a_n x^2 + 2b_n x\bar{p}_x + c_n \bar{p}_x^2 + 2d_n xy + 2e_n x\bar{p}_y \\
&+ 2f_n y\bar{p}_x + 2g_n \bar{p}_x \bar{p}_y + u_n y^2 + 2v_n y\bar{p}_y + w_n \bar{p}_y^2)\bar{\delta}^n/2 \\
&\equiv (Ax^2 + 2Bx\bar{p}_x + C\bar{p}_x^2 + 2Dxy + 2Ex\bar{p}_y \\
&+ 2Fy\bar{p}_x + 2G\bar{p}_x\bar{p}_y + Uy^2 + 2Vy\bar{p}_y + W\bar{p}_y^2)/2, \qquad (55)
\end{aligned}
$$

where the coefficients D to W have the similar forms as those shown in Eq. (47). It is obvious that the 10 sets of coefficients $a_n, ..., w_n$ are related to the chromatic aberrations $\alpha_{x,n}$, $\beta_{x,n}$, $\mu_{x,n}$, $\alpha_{y,n}$, $\beta_{y,n}$, $\mu_{y,n}$, and $r_{i,n}$, $i = 1, ..., 4$. The transformation due to the Hamiltonian is expressed in the same manner as in Eqs. (34)−(37)

$$\bar{x} = x + \frac{\partial H_\xi}{\partial \bar{p}_x} = x + Bx + C\bar{p}_x + Fy + G\bar{p}_y, \qquad (56)$$

$$p_x = \bar{p}_x + \frac{\partial H_\xi}{\partial x} = \bar{p}_x + Ax + B\bar{p}_x + Dy + E\bar{p}_y, \qquad (57)$$

$$\bar{y} = y + \frac{\partial H_\xi}{\partial \bar{p}_y} = y + Vy + W\bar{p}_y + Ex + G\bar{p}_x, \qquad (58)$$

$$p_y = \bar{p}_y + \frac{\partial H_\xi}{\partial y} = \bar{p}_y + Uy + V\bar{p}_y + Dx + F\bar{p}_x, \qquad (59)$$

$$
\begin{aligned}
\bar{z} = z + \frac{\partial H_\xi}{\partial \bar{\delta}} &= z + x^2 \sum_n n a_n \bar{\delta}^{n-1}/2 + x\bar{p}_x \sum_n n b_n \bar{\delta}^{n-1} \\
&+ \bar{p}_x^2 \sum_n n c_n \bar{\delta}^{n-1}/2 + xy \sum_n n d_n \bar{\delta}^{n-1} + x\bar{p}_y \sum_n n e_n \bar{\delta}^{n-1} \\
&+ \bar{p}_x y \sum_n n f_n \bar{\delta}^{n-1} + \bar{p}_x \bar{p}_y \sum_n n g_n \bar{\delta}^{n-1} + y^2 \sum_n n u_n \bar{\delta}^{n-1}/2 \\
&+ y\bar{p}_y \sum_n n v_n \bar{\delta}^{n-1} + \bar{p}_y^2 \sum_n n w_n \bar{\delta}^{n-1}/2, \qquad (60)
\end{aligned}
$$

$$\delta = \bar{\delta}. \qquad (61)$$

The above equations represent an implicit map for the chromatic aberrations, its explicit form can be found after tedious calculations, resulting in a 4×4 matrix of $M_H(\delta)$ as follows:

$$
\begin{aligned}
M_{H,11} &= 1 + B + CM_{H,21} + GM_{H,41}, \\
M_{H,12} &= \frac{C - FG + CV}{K}, \\
M_{H,13} &= F + CM_{H,23} + GM_{H,43}, \\
M_{H,14} &= \frac{G - CE + BG}{K}, \\
M_{H,21} &= \frac{-A + DE - AV}{K}, \\
M_{H,22} &= \frac{1 + V}{K},
\end{aligned}
$$

$$
\begin{aligned}
M_{H,23} &= -\frac{D - EU + DV}{K},\\
M_{H,24} &= -\frac{E}{K},\\
M_{H,31} &= E + WM_{H,41} + GM_{H,21},\\
M_{H,32} &= \frac{G + GV - FW}{K},\\
M_{H,33} &= 1 + V + WM_{H,43} + GM_{H,23},\\
M_{H,34} &= \frac{W - EG + BW}{K},\\
M_{H,41} &= -\frac{D + BD - AF}{K},\\
M_{H,42} &= -\frac{F}{K},\\
M_{H,43} &= \frac{-U + DF - BU}{K},\\
M_{H,44} &= \frac{1 + B}{K},
\end{aligned}
\tag{62}
$$

where $K = (1 + B)(1 + V) - EF$. The relations between the Twiss parameters $(\alpha_n, ..., r_i)$ and the coefficients $(a_n, ..., w_n)$ are determined by

$$M_4(\delta) = M_4(0)M_H(\delta). \tag{63}$$

The left-hand side (LHS) and the RHS of the above equation are expressed using the Twiss parameters and coefficients of the Hamiltonian, respectively. It is very complicated to write down the analytical expressions for the relations between the chromatic aberrations and the coefficients of the Hamiltonian. However, it is easy to obtain these relationships numerically. Multiplying Eq. (63) with $M(0)^{-1}$, we have

$$M_4(0)^{-1}M_4(\delta) = M_H(\delta). \tag{64}$$

The RHS of the above equation can be expanded in terms of δ as follows:

$$M_H(\delta) = \sum_{n=1} M_{H,n}\delta^n. \tag{65}$$

The first and second matrix coefficients are

$$M_{H,1} = \begin{pmatrix} b_1 & c_1 & f_1 & g_1 \\ -a_1 & -b_1 & -d_1 & -e_1 \\ e_1 & g_1 & v_1 & w_1 \\ -d_1 & -f_1 & -u_1 & -v_1 \end{pmatrix}, \tag{66}$$

$$M_{H,2} = \begin{pmatrix} b_2 - a_1c_1 - d_1g_1 & c_2 - b_1c_1 - f_1g_1 & f_2 - c_1d_1 - g_1u_1 & g_2 - c_1e_1 - g_1v_1 \\ -a_2 + a_1b_1 + d_1e_1 & -b_2 + b_1^2 + e_1f_1 & -d_2 + b_1d_1 + e_1u_1 & -e_2 + b_1e_1 + e_1v_1 \\ e_2 - a_1g_1 - d_1w_1 & g_2 - b_1g_1 - f_1w_1 & v_2 - d_1g_1 - u_1w_1 & w_2 - e_1g_1 - v_1w_1 \\ -d_2 + a_1f_1 + d_1v_1 & -f_2 + b_1f_1 + f_1v_1 & -u_2 + d_1f_1 + u_1v_1 & -v_2 + e_1f_1 + v_1^2 \end{pmatrix}.$$

Note that $M_{H,1}$ contains only first-order coefficients of the Hamiltonian, and the elements of $M_{H,2}$ contains second-order coefficients and products of first-order coefficients. Thus, all coefficients are determined uniquely. The form of $M_{H,3}$ is similar to that of $M_{H,2}$ but is not shown here due to its huge size.

On the other hand, the LHS of Eq. (64) can be expanded in terms of δ as follows:

$$M_4(0)^{-1}M_4(\delta) = I_4 + \sum_{n=1} M_n\delta^n, \tag{67}$$

where M_n is numerically defined for the given chromatic aberrations, $\alpha_{x,n}$, $\beta_{x,n}$, $\mu_{x,n}$, $\alpha_{y,n}$, $\beta_{y,n}$, $\mu_{y,n}$, and $r_{i,n}$, $i = 1, ..., 4$. The coefficients can be determined order-by-order. Now, we determine $10 \times n$ independent coefficients of the Hamiltonian H_I from the chromatic aberrations in tunes, Twiss parameters, and x-y coupling. A symplectic transformation for the Hamiltonian is obtained from Eqs. (62) and (60) using the observed or computed chromatic aberrations, $\alpha_{x,n}$, $\beta_{x,n}$, $\mu_{x,n}$, $\alpha_{y,n}$, $\beta_{y,n}$, $\mu_{y,n}$, and $r_{i,n}$, $i = 1, ..., 4$. A one-turn map is again obtained via Eq. (44).

3.4. *Direct method for chromatic aberrations*

In the previous sections, the Hamiltonian is used to construct a perturbation map for chromatic aberrations. Since the Hamiltonian is written in the truncated form of power series in terms of momentum deviation, there is leakage in high-order chromatic aberrations. Actually, the map for chromatic aberrations can be directly obtained without using either a Hamiltonian or a generating function. This direct map is also symplectic in the six-dimensional phase space and strictly reproduces the chromatic aberrations. That is, there is no leakage to higher-order terms in δ, in contrast to what are reported in §§3.1–3.3.

Given that the transfer matrix for the betatron motion depends on δ, to satisfy the symplectic condition, the longitudinal coordinate z should be mapped with a function of the betatron and synchrotron variables as follows:

$$\bar{\boldsymbol{x}} = M_4(\delta)\boldsymbol{x}, \tag{68}$$

$$\bar{z} = z + g(x, p_x, y, p_y, z, \delta), \tag{69}$$

$$\delta = \bar{\delta}, \tag{70}$$

where $M_4(\delta)$ will generally have the same form of Eq. (53). Mathematically, the symplectic map should satisfy the following Poisson bracket relation:

$$[\bar{x}, \bar{z}] = [\bar{p_x}, \bar{z}] = [\bar{y}, \bar{z}] = [\bar{p_y}, \bar{z}] = 0, \tag{71}$$

$$[\bar{z}, \bar{\delta}] = 1. \tag{72}$$

Equation (72) requires g to be independent of z, because $[z + g, \delta] = 1$ gives $\partial_z g = 0$. Equation (71) is expressed in matrix form of

$$[M_4(\delta)\boldsymbol{x}, z] + [M_4(\delta)\boldsymbol{x}, g(x, p_x, y, p_y, \delta)] = 0. \tag{73}$$

The explicit expression of the Poisson bracket is

$$(\partial_\delta M_4(\delta))\boldsymbol{x} + M_4(\delta)S_4(\partial_{\boldsymbol{x}} g) = 0, \tag{74}$$

where $\partial_{\boldsymbol{x}} g = (\partial_x g, \partial_{p_x} g, \partial_y g, \partial_{p_y} g)^T$ and

$$S_4 = \begin{pmatrix} S_2 & 0 \\ 0 & S_2 \end{pmatrix}. \tag{75}$$

By using the symplectic condition for M_4, one can obtain the following result from Eq. (74)

$$\partial_{\boldsymbol{x}} g = M_4^T(\delta) S_4 (\partial_\delta M_4(\delta)) \boldsymbol{x}. \tag{76}$$

Performing differentiation with respect to δ to the symplectic condition for M_4 leads to

$$\begin{aligned} \partial_\delta (M_4^T(\delta) S_4 M_4(\delta)) &= (\partial_\delta M_4^T(\delta)) S_4 M_4(\delta) \\ &\quad + M_4^T(\delta) S_4 (\partial_\delta M_4(\delta)) = 0. \end{aligned} \tag{77}$$

Equation (77) shows that $M_4^T S_4 (\partial_\delta M_4)$ is a symmetric matrix. Therefore, g is obtained from Eq. (76) as

$$g = \boldsymbol{x}^T M_4^T(\delta) S_4 (\partial_\delta M_4(\delta)) \boldsymbol{x}/2. \tag{78}$$

The term that depends only on δ appears as nonlinear momentum compaction in the next section.

Here we show the expression for g in more detail. $\partial_\delta M_4(\delta)$ is given by

$$\begin{aligned} \partial_\delta M_4(\delta) &= \partial_\delta (R(\delta) M_{2\times 2}(\delta) R^{-1}(\delta)) \\ &= \partial_\delta R M_{2\times 2} R^{-1} + R \partial_\delta M_{2\times 2} R^{-1} + R M_{2\times 2} \partial_\delta R^{-1}, \end{aligned} \tag{79}$$

where $\partial_\delta M_{2\times 2}$ is represented by $\partial_\delta M_{x,y}$. And $\partial_\delta M_{x,y}(\delta)$ is expressed by

$$\partial_\delta M_i(\delta) = \begin{pmatrix} -\partial_\delta \mu_i \sin\mu_i + \partial_\delta \alpha_i \sin\mu_i + \alpha_i \partial_\delta \mu_i \cos\mu_i & \partial_\delta \beta_i \sin\mu_i + \beta_i \partial_\delta \mu_i \cos\mu_i \\ -\partial_\delta \gamma_i \sin\mu_i - \gamma_i \partial_\delta \mu_i \cos\mu_i & -\partial_\delta \mu_i \sin\mu_i - \partial_\delta \alpha_i \sin\mu_i - \alpha_i \partial_\delta \mu_i \cos\mu_i \end{pmatrix}, \tag{80}$$

where

$$\partial_\delta \gamma_i = \frac{2\partial_\delta \alpha_i \alpha_i}{\beta_i} - \frac{1+\alpha_i^2}{\beta_i^2} \partial_\delta \beta_i, \quad i = x, y. \tag{81}$$

In the case of $\partial_\delta R$, the derivative for $r_0 = \sqrt{1 - r_1 r_4 + r_2 r_3}$ is obtained in the same manner as Eq. (81).

This direct method can be straightforwardly extended to the transfer map for off-momentum particles between two arbitrary positions s_1 and s_2 around the ring. Assuming that the RF cavity is not located between s_1 and s_2, the map can be written in the form of

$$\boldsymbol{x}(s_2) = M_4(s_2, s_1, \delta) \boldsymbol{x}(s_1), \tag{82}$$

$$z(s_2) = z(s_1) + g\Big(x(s_1), p_x(s_1), y(s_1), p_y(s_1), z(s_1), \delta\Big) \tag{83}$$

with g given by

$$g = \boldsymbol{x}(s_1)^T M_4^T(s_2, s_1, \delta) S_4 (\partial_\delta M_4(s_2, s_1, \delta)) \boldsymbol{x}(s_1)/2, \tag{84}$$

where $M_4(s_2, s_1, \delta) = R(s_2, \delta) M_{2\times 2}(s_2, s_1, \delta) R(s_1, \delta)^{-1}$. The matrix elements are written in the form of Twiss parameters and phase advance between s_1 and s_2 in terms of the power series of δ.

3.5. *Nonlinear dispersion*

The symplectic map for nonlinear dispersion can be derived in a similar way. For the sake of simplicity we neglect the chromatic aberrations in $\zeta_{x,y}, \zeta'_{x,y}$ in this section. It is also assumed that the 0th-order terms of $\zeta_{x,y}$ and $\zeta'_{x,y}$ with respect to δ have already been subtracted from $\boldsymbol{x}$, as shown in §2.1. First we assume that the nonlinear dispersion contribution is subtracted from the betatron coordinates as follows:

$$\boldsymbol{x}_{\beta_N} = \boldsymbol{x}_\beta - \sum_{n=2} \boldsymbol{\eta}_n \delta^n, \tag{85}$$

where $\boldsymbol{x}_{\beta_N}$ is the betatron coordinate around the δ-dependent closed orbit. The subscript $_\beta$ is again used for the betatron variables. From Eq. (85), the related Hamiltonian is described by

$$S_4 \frac{\partial H_\eta}{\partial \boldsymbol{x}_{\beta_N}} = \sum_{n=2} \boldsymbol{\eta}_n \delta^n. \tag{86}$$

The above equation can be integrated over the coordinates to obtain the Hamiltonian as follows:

$$H_\eta = \sum_{n=2} (\eta'_{x,n} x_{\beta_N} - \eta_{x,n} p_{x,\beta_N} + \eta'_{y,n} y_{\beta_N} - \eta_{y,n} p_{y,\beta_N}) \delta^n. \tag{87}$$

This Hamiltonian gives the transformations expressed by Eq. (85) and the following transformation for the longitudinal coordinate:

$$z_{s_N} = z_s + \sum_{n=2} (\eta'_{x,n} x_{\beta_N} - \eta_{x,n} p_{x,\beta_N} + \eta'_{y,n} y_{\beta_N} - \eta_{y,n} p_{y,\beta_N}) n \delta^{n-1}. \tag{88}$$

Suppose the transformation described by Eqs. (85) and (88) equals $\mathcal{M}_{H_\eta}$, the one-turn map is now expressed by

$$R_\eta \circ \mathcal{M}_{H_\eta}^{-1} \circ M_{4\times 2}(0) \circ \mathcal{M}_{H_I} \circ \mathcal{M}_{H_\eta} \circ R_\eta^{-1} \circ \boldsymbol{x}. \tag{89}$$

Similarly, the nonlinear momentum compaction can also be introduced in the same way as the nonlinear dispersion. Suppose that the related Hamiltonian is

$$H_{\alpha_p} = \sum_{n=3} \frac{\alpha_{p,n}}{n!} \delta^n, \tag{90}$$

where $\alpha_{p,n}$ is the n-th order momentum compaction with respect to δ. Then, replacing H_η by $H_\eta + H_{\alpha_p}$ in Eq. (89) gives the symplectic map including the effects of both nonlinear dispersions and momentum compactions.

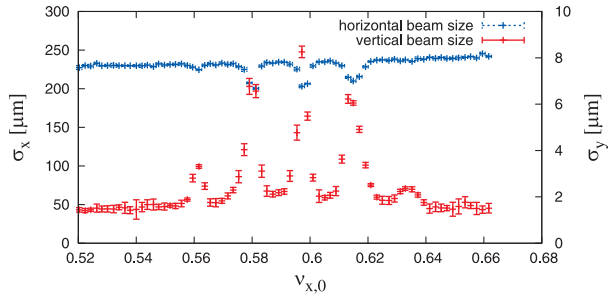

Fig. 2. Measured vertical and horizontal beam sizes. The red crosses denote the vertical beam size and the blue crosses denote the horizontal beam size. The vertical beam size around the non-resonance point is approximately 1.25μm. The vertical and longitudinal tunes are $\nu_y = 0.6$ and $\nu_z = -0.021$, respectively.

§4. Synchro-betatron resonances driven by chromatic aberrations in KEKB

As seen in the previous section, the Hamiltonian related to chromatic aberrations represents a quadratic form with respect to the betatron variables and a form of power series with respect to the momentum deviation. The symplectic map derived from the Hamiltonian clearly indicates the coupling of betatron and synchrotron motions, and thence synchro-betatron resonances can be studied straightforwardly. In this section, we compare the measurements with simulations related to synchro-betatron resonances in KEKB.

In the KEKB, two types of measurements were performed to study chromatic aberrations. One was a beam size measurement versus transverse tune. The second was the measurement of chromatic aberrations at the interaction point using turn-by-turn data obtained with beam position monitors.

The beam size is measured with a synchrotron light monitor using an interferometer.[14] Figure 2 shows the transverse beam size versus the horizontal tune measured on May 16, 2008 for $\nu_y = 0.6$ and $\nu_z = -0.021$. Several peaks can be observed in the figure, and their positions are shifted as ν_y was varied. This indicates that the peaks corresponds to the linear x-y coupling resonance and its synchrotron sidebands. This measurement confirmed the existence of remarkable chromatic aberrations in KEKB optics. Similar measurements were also performed at CESR.[15]

The chromatic aberrations for optics parameters at the interaction point are measured using turn-by-turn data obtained with beam position monitors located on both sides of the interaction point ($s = \pm 0.7$ m) for various values of beam energy.[2),3)] They are measured in a single-bunch operation without collisions. Table I lists the values of the chromatic aberrations measured on May 26, 2009. It is difficult to precisely measure the vertical Twiss parameters (β_y, α_y) at the interaction point;[*)]

[*)] The vertical beta function at the interaction point is determined by $\beta_y = (\beta_{y,m} - \sqrt{\beta_{y,m}^2 - 4s^2})/2$, where $\beta_{y,m}$ is the beta function of the monitor. The beta function at the interaction point β_y is given by the difference between two large values.

Table I. Chromatic aberrations in linear optics parameters measured at the KEKB interaction point; the values for α_y and β_y were obtained by SAD using the design lattice.

	β_x	α_x	β_y(SAD)	α_y(SAD)	ν_x	ν_y	r_1	r_2	r_3	r_4
δ^0	1.31	0.00482	0.00590	3.81×10^{-5}	0.526	0.588	0	0	0	0
δ^1	0.890	5.46	-0.109	22.2	1.60	4.75	0.0235	-0.737	-38.8	-84.0
δ^2	2.12×10^3	-2.56×10^3	6.06	-1.58×10^3	112	52.1	263	-235	2.33×10^4	-1.26×10^4
δ^3	-2.50×10^5	9.67×10^5	-0.659	-58.3	2.38×10^3	-1.54×10^4	2.64×10^4	2.48×10^4	-7.65×10^5	5.48×10^5

Table II. Coefficients of the Hamiltonian obtained by the method described in §3.3 using the chromatic aberrations in Table I for $\nu_{x,0} = 0.526$ and $\nu_{y,0} = 0.588$.

	a	b	c	d	e	f	g	u	v	w
δ^1	7.51	0.902	13.5	25.1	-0.160	-57.6	-0.404	0.543×10^4	15.0	0.164
δ^2	392	-339	0.131×10^4	0.238×10^5	85.3	-0.157×10^5	-145	0.216×10^6	406	4.11
δ^3	-361	0.110×10^6	0.806×10^5	0.193×10^7	0.370×10^5	0.208×10^8	0.256×10^5	-0.173×10^8	-0.387×10^5	-430

therefore, the values computed by SAD[16] for the design lattice were used. These values changed after every optics correction (performed after each machine break, which occurs once in two or three weeks) and every beam tuning of optimizing the luminosity (performed day by day).

The coefficients of the Hamiltonian H_I for the chromatic aberrations are calculated up to the third order using the method described in §3.3, and the values are listed in Table II.

The synchro-betatron resonances caused by the chromatic aberrations were studied using the symplectic map expressed by the Hamiltonian H_I. A particle-tracking code based on the formalism described in §3.3 was written and used to track particles in the presence of the measured chromatic aberrations. In the simulations, 1000 macroparticles are initialized with a Gaussian distribution in which the initial size is given by the emittance and linear optics parameters, where the horizontal, vertical, and longitudinal emittances are $\epsilon_x = 1.8 \times 10^{-8}$ m, $\epsilon_y = 1.8 \times 10^{-10}$ m and $\epsilon_z = 4.9 \times 10^{-6}$ m, respectively. The macroparticles are tracked with radiation damping (4000/2000 turns in transverse/longitudinal directions, respectively) and excitation. The equilibrium beam sizes in the horizontal and vertical planes are obtained by taking the average of the particle coordinates after 30,000 turns.

The horizontal tune is scanned in steps of $\Delta\nu_x = 1.4 \times 10^{-4}$ at a fixed vertical tune $\nu_y = 0.588$; the coefficients in the Hamiltonian H_I are kept constant during the tune scan. We also assume that the 0th-order x-y coupling parameters vanish because they are optimized during the daily operation at KEKB. Figure 3 shows the resulting beam sizes normalized by the unperturbed beam size. Dispersion is not taken into account in this simulation, that is, $R_\eta = I_6$. It is seen that several peaks in the beam sizes are observed in the figure. They correspond to the synchro-betatron resonances generated at $\ell\nu_x + m\nu_y + n\nu_z = Integer$, with ℓ, m, and n integers. Each resonance is characterized by the values of (ℓ, m, n), and the peaks from left to right in Fig. 3 correspond to the following resonances: (2,0,1), (1,−1,−3), (1,−1,−2), (1,−1,−1), (1,−1,0), (1,−1,1) and (1,−1,2). At the resonance of $2\nu_x + \nu_z = Integer$, both the horizontal and the vertical beam sizes increase. Essentially, these reso-

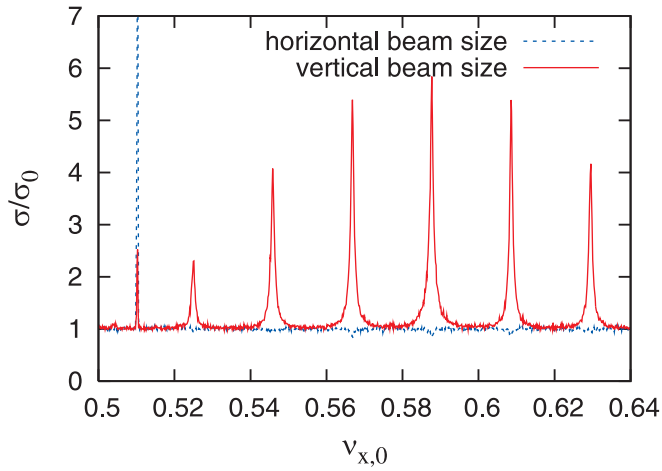

Fig. 3. Simulated vertical and horizontal beam sizes versus unperturbed horizontal tune, obtained using coefficients up to the third order in the Hamiltonian. Vertical and longitudinal tunes are $\nu_y = 0.588$ and $\nu_z = -0.021$, respectively.

nances cause the horizontal beam size to blow up. The vertical beam size increases because of the nonlinear x-y coupling due to the chromatic aberrations. At the synchrotron sideband resonance of the x-y coupling, the vertical beam size increases but the horizontal beam size decreases. These behaviors qualitatively agree with the measurements shown in Fig. 2. It is also noted that the width of the simulated peak is narrower than that of the measurement result. There are various uncertainties in the beam measurements, such as higher-order optics and measurement conditions. For example, the beam size measurement took around 1 min at each frequency, so the tune drift may affect the measured spread.

The damping time of the betatron oscillation has been measured to be 2000−4000 turns, which is consistent with the radiation damping time given by SAD. The corresponding tune shift is less than 0.0005. The nonlinear terms in the Hamiltonian such as $x^m y^n$ with $m + n \geq 4$ are estimated to be very small at KEKB, thus their effect on the tune spread should be negligible. The spread of the sideband can be induced by higher-order nonlinear terms, such as $x^m y^n \delta$. Linear x-y coupling is controlled at the operating point around $(\nu_x, \nu_y) = (0.51, 0.56)$ but not at other points in the tune scan measurement. Ambiguity in the measurement, linear x-y coupling, or nonlinear chromatic coupling are plausible explanations for the width discrepancy in the present result.

§5. Conclusions

Chromatic aberrations characterize how the linear optics parameters of betatron oscillation vary under slow synchrotron oscillation. In most circular accelerators, the optics parameters depend only on the momentum deviation δ. The transverse oscillation, which depends on δ, produces (because of betatron oscillation) an effect

in z, which is a canonical conjugate of δ. Both the transverse oscillation and the effect on z maintain symplecticity in a six-dimensional phase space.

In this paper, we have discussed the symplectic expressions for chromatic aberrations. The main properties of our method are summarized as follows: 1) It utilizes the measurement of optics parameters as power series of the momentum deviation; 2) It assumes that the Courant-Snyder formalism can be extended to the off-momentum particles; 3) The revolution matrix in the four-dimensional betatron phase space can be written in the form of power series of the momentum deviation; 4) The symplectic condition is enforced and thus the one-turn symplectic map is constructed in the six-dimensional phase space.

Using two methods, the six-dimensional symplectic map is obtained from four-dimensional revolution matrix. The first method is based on a Hamiltonian formalism using the generating function, which yields six-dimensional canonical transformations. The second method is based on matrix transformation with an additional longitudinal transformation so as to retain the symplectic condition. These methods can be applied to construction of symplectic maps between two arbitrary locations in a ring.

Contemporary circular machines are equipped with many turn-by-turn monitors. The Twiss parameters and phase advances can be measured at many places in the ring; therefore, transfer maps with chromatic aberrations can be obtained at the places. These methods can treat extended chromatic aberrations, i.e. the optics parameters in the betatron matrix $M_4(z, \delta)$ are functions of both momentum deviation and longitudinal position. For instance, the first method can straightforwardly treat $M_4(z, \delta)$ up to a second-order polynomial of z and δ.

The symplectic map can be used in six-dimensional particle tracking simulations for purpose of studying the influence of chromatic aberrations on synchro-beta resonances with beam-beam, space charge, impedance effects, and so on. The synchro-beta resonance case was studied to demonstrate the capability of the obtained symplectic map. Results of particle tracking simulation using the symplectic expression were compared with beam size measurements in tune space. Simulation results qualitatively agreed with the measurements of resonance behavior.

Acknowledgements

The authors thank Dr. E. Perevedentsev for providing the motivation to write this paper. Sincere thanks are due to Drs. H. Koiso, S. Kamada, K. Oide, and Y. Cai for fruitful discussions. The authors also greatly appreciate Dr. E. Forest for making many valuable suggestions.

References

1) G. Arduini, R. Tomas, F. Zimmermann, A. Faus-Golfe and N. Iida, PAC03-WPAB084, CERN-AB-2003-030-ABP, May 2003.
2) Y. Ohnishi, K. Ohmi, H. Koiso, M. Masuzawa, A. Morita, K. Mori, K. Oide, Y. Seimiya and D. Zhou, Phys. Rev. ST Accel. Beams **12** (2009), 091002.
3) K. Ohmi, T. Ieiri, Y. Ohnishi, Y. Seimiya, M. Tobiyama and D. Zhou, *Proceedings of IPAC10, Kyoto* (2010).

4) "KEKB B-Factory design report", KEK-Report-95-7 (1995).
K. Ohmi, *Proceedings of EPAC2000* (2000), p. 435.
5) A. Morita, H. Koiso, Y. Ohnishi and K. Oide, Phys. Rev. ST Accel. Beams **10** (2007), 072801.
6) D. Zhou, K. Ohmi, Y. Seimiya, Y. Ohnishi, A. Morita and H. Koiso, Phys. Rev. ST Accel. Beams **13** (2010), 021001.
7) Y. Funakoshi et al., to be published.
8) K. Ohmi, K. Hirata and K. Oide, Phys. Rev. E **49** (1994), 751.
9) L. Teng, *Concerning n-Dimensional Coupled Motions*, FN-229 (1971).
D. A. Edwards and L. C. Teng, IEEE Trans. Nucl. Sci. **20** (1973), 885.
10) K. Yokoya, private communications.
This formalism is a correction of Edwards and Teng's formalism, i.e., $r_0 > 1$ is possible for $\det(R_2) < 0$.
11) E. Forest, *Beam Dynamics: A New Attitude and Framework* (Harwood Academic Publishers, 1998).
12) Y. Yan, *Applications of differential algebra to single-particle dynamics in storage ring*, SSCL-500 (1991).
13) H. Goldstein, C. Poole and J. Safko, *Classical Mechanics*, 3rd edition (Addison Wesley, 2002), p. 385.
14) J. W. Flanagan, S. Hiramatsu and T. Mitsuhashi, *Proceedings of European Particle Accelerator Conference (EPAC2000)* (2000), p. 1783.
15) A. Temnykh, *Proceedings of Factories 2008.*
16) `http://acc-physics.kek.jp/SAD/`